

Supplementary Materials

Grid Independence Test

In the VOF numerical calculation, grid size is especially important in the region where the contact angle plays a major role. Coarse grids may cause larger discretization errors, while the refined meshes could reduce numerical errors. However, as the mesh becomes finer, the number of meshes exponentially increases and the calculation time also drastically increases. Thus, mesh should have appropriate sizing. The results calculated by a proper grid number could be close to the experimental data. The structured grid was used for the simulation. The independence test of the structured grid was carried out on the coating fluid model. Numerical simulations with the mesh numbers of 3040, 4332, 5050, 7200, 9918, 12,606, 18,400, 25,803, 28,028, 40,533, 50,490, and 79,431 were performed, respectively. The static contact angle of substrate surface and sides was 90° . To investigate the grid independence, the maximum height (h) of the surface unevenness was measured at $20 \mu\text{s}$. This measured value was divided by the initial height of the coating fluid (h_0) to express the values as dimensionless variables. As shown in Figure S1, when the grid number was larger than 25,803, the results of maximum height converged. Therefore, the grid number of 28,028 was chosen in our numerical simulation.

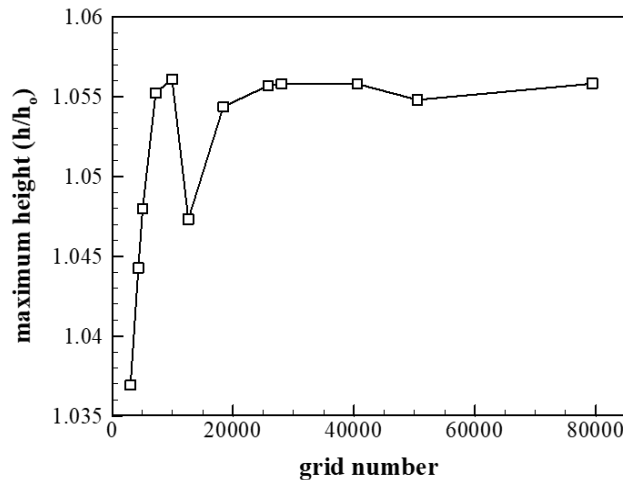


Figure S1. Variation of the maximum height of the surface unevenness with the grid number.

The time and grid convergence test was checked by the Courant–Friedrichs–Lewy (CFL) number [42]. The CFL number indicates that the distance of information travels during the time step should be lower than the distance between the mesh element. In this point, CFL number should be lower than 1,

$$CFL = \frac{a \cdot \Delta t}{\Delta x} \leq 1 \quad (1)$$

where “ a ” is the velocity magnitude (m/s), “ Δt ” is the computational time step (s), and “ Δx ” is the distance between mesh elements (m). In our simulation model, the time step was $0.1 \mu\text{s}$ and the distance between mesh elements was $2 \mu\text{m}$. The maximum velocity magnitude under the same wetting condition of 90° was 0.855 m/s at $100 \mu\text{s}$. In our simulation case, the CFL condition number was 0.04275 . Therefore, our numerical simulation model and grid satisfied the grid and time convergence test.

Validation of the Numerical Model

To validate the numerical model, the contact angles on a silicon wafer substrate were compared with the results of the surface contact angle simulation. Water contact angles of the sessile droplets were measured on the silicon wafer substrate using 4 μL droplets at an ambient temperature. Digital images were obtained using a charge coupled device camera (PCO4000, PCO AG). The silicon wafer substrate showed the average static contact angle of 66.2° . To compare this result, numerical simulations were conducted using 4 μL at the ambient temperature condition. The water had a density of 1000 kg/m^3 , a dynamic viscosity of 0.001 kg/ms , and a surface tension of 0.0725 N/m . It was assumed that the coating fluid and substrate were surrounded by gas (air) at room temperature (25°C) and ambient pressure ($101,325 \text{ Pa}$). The gas density was set to 1.1614 kg/m^3 , and its dynamic viscosity was set to $1.846 \times 10^{-5} \text{ kg/ms}$. The computational time step of the simulation model was $0.1 \mu\text{s}$. The structured grid was used for the simulation. Figure S2 shows the comparison between the static contact angle of the silicon wafer and the simulation result of the contact angle. The contact angle of the simulation results was 64.9° . These results show that the simulation is in reasonable agreement with the experiment data. Therefore, our numerical model is considered accurate enough to examine the coating fluid surface in terms of the substrate contact angle.

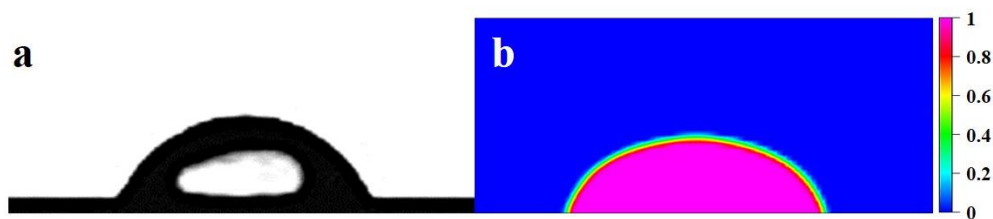


Figure S2. Comparison between the (a) static contact angle of the silicon wafer and (b) the simulation result of the contact angle.

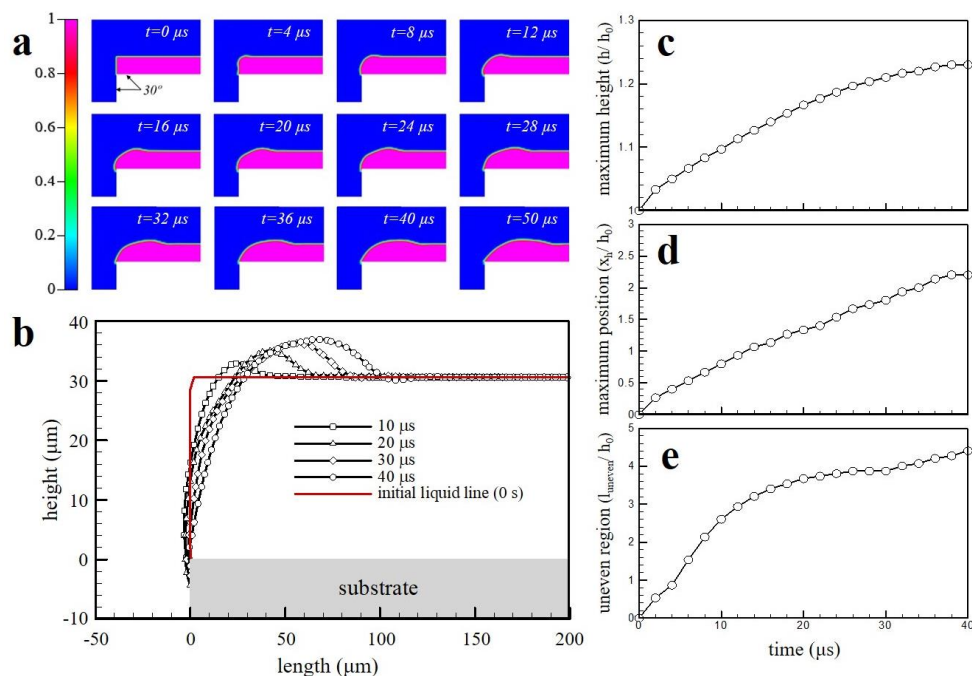


Figure S3. (a) Coating fluid behavior over time at the edge of the substrate under the same wetting condition of 30° , (b) surface profile under the same wetting condition of 30° , (c) maximum height, (d) maximum position, and (e) uneven region analysis of the surface unevenness at the edge of substrate under the same wetting condition of 30° .

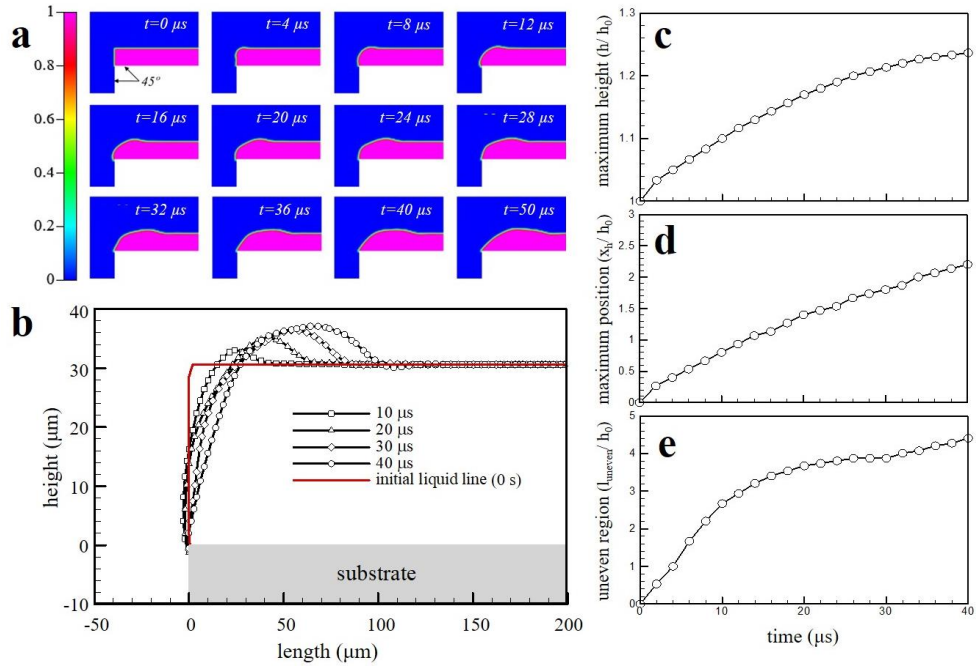


Figure S4. (a) Coating fluid behavior over time at the edge of the substrate under the same wetting condition of 45° , (b) surface profile under the same wetting condition of 45° , (c) maximum height, (d) maximum position, and (e) uneven region analysis of the surface unevenness at the edge of substrate under the same wetting condition of 45° .

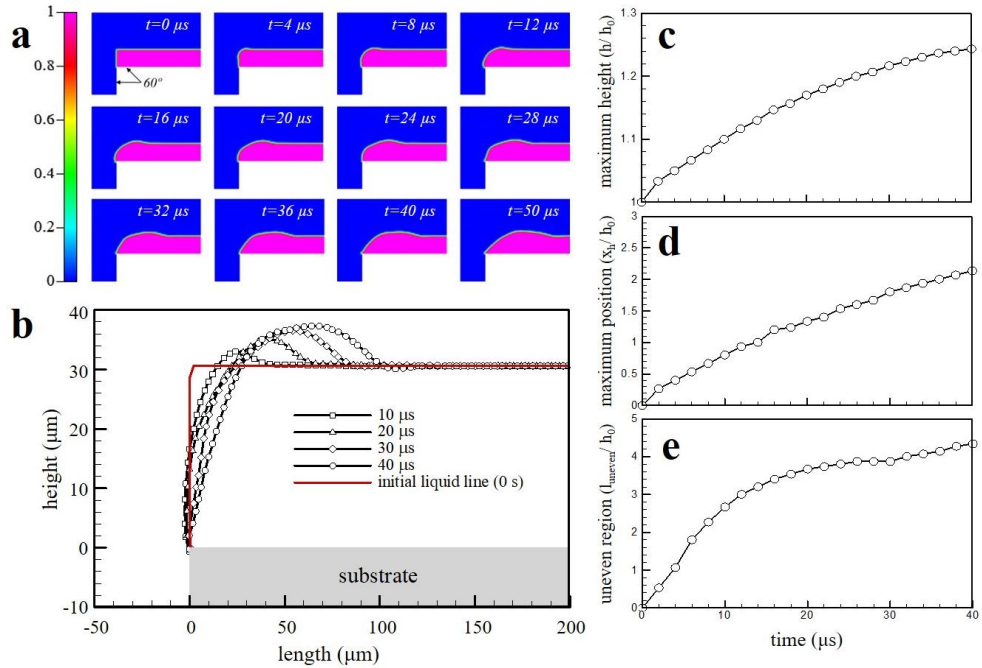


Figure S5. (a) Coating fluid behavior over time at the edge of the substrate under the same wetting condition of 60° , (b) surface profile under the same wetting condition of 60° , (c) maximum height, (d) maximum position, and (e) uneven region analysis of the surface unevenness at the edge of substrate under the same wetting condition of 60° .

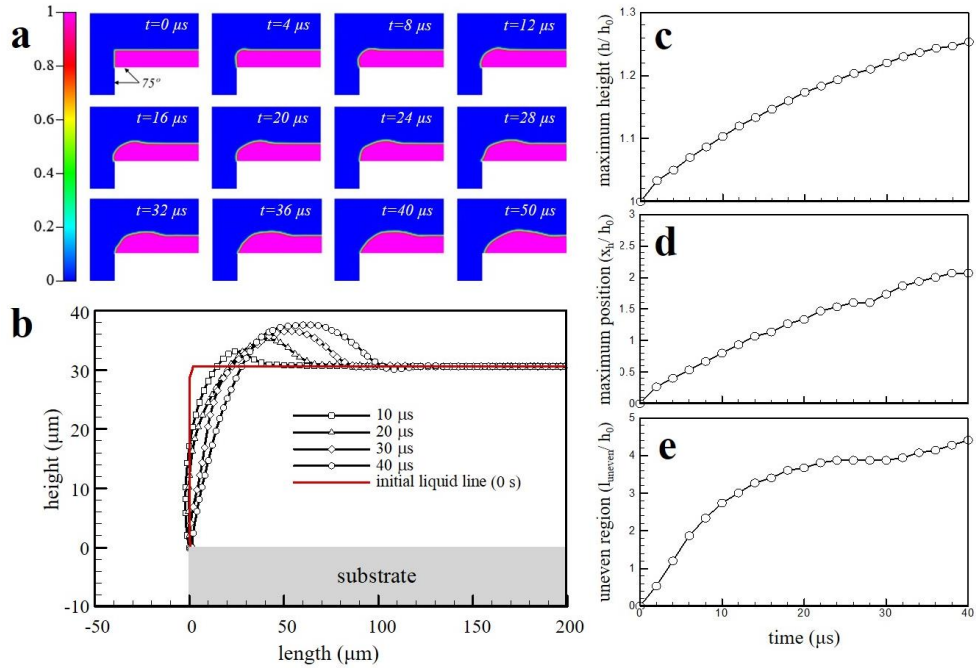


Figure S6. (a) Coating fluid behavior over time at the edge of the substrate under the same wetting condition of 75° , (b) surface profile under the same wetting condition of 75° , (c) maximum height, (d) maximum position, and (e) uneven region analysis of the surface unevenness at the edge of substrate under the same wetting condition of 75° .

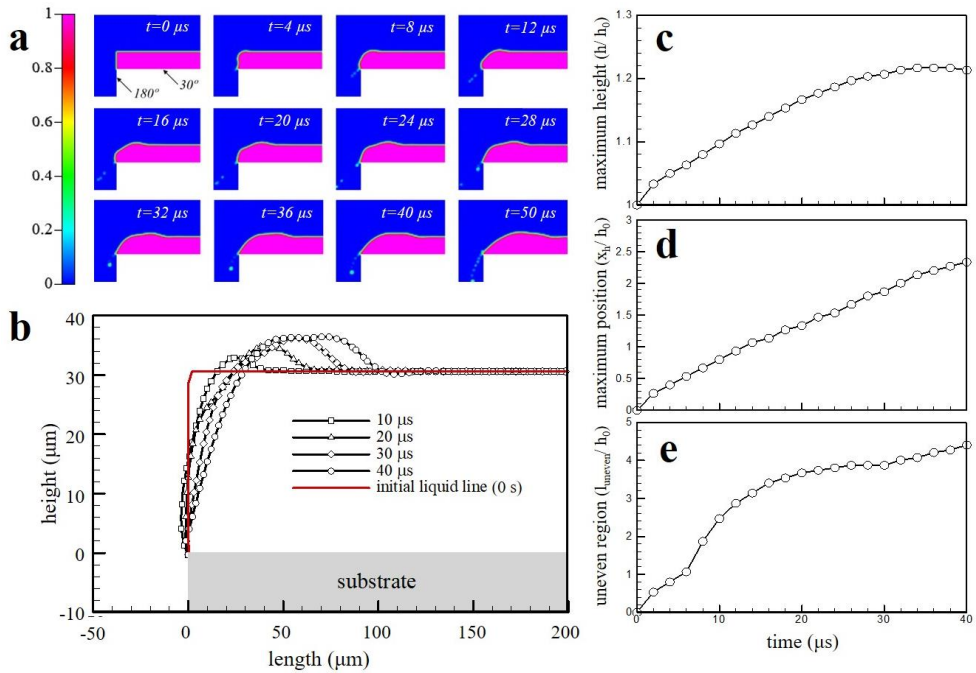


Figure S7. (a) Coating fluid behavior over time at the edge of the substrate under a substrate surface contact angle of 30° and a side contact angle of 180° , (b) surface profile under the different wetting condition, (c) maximum height, (d) maximum position, and (e) uneven region analysis of the surface unevenness at the edge of substrate under the different wetting condition.

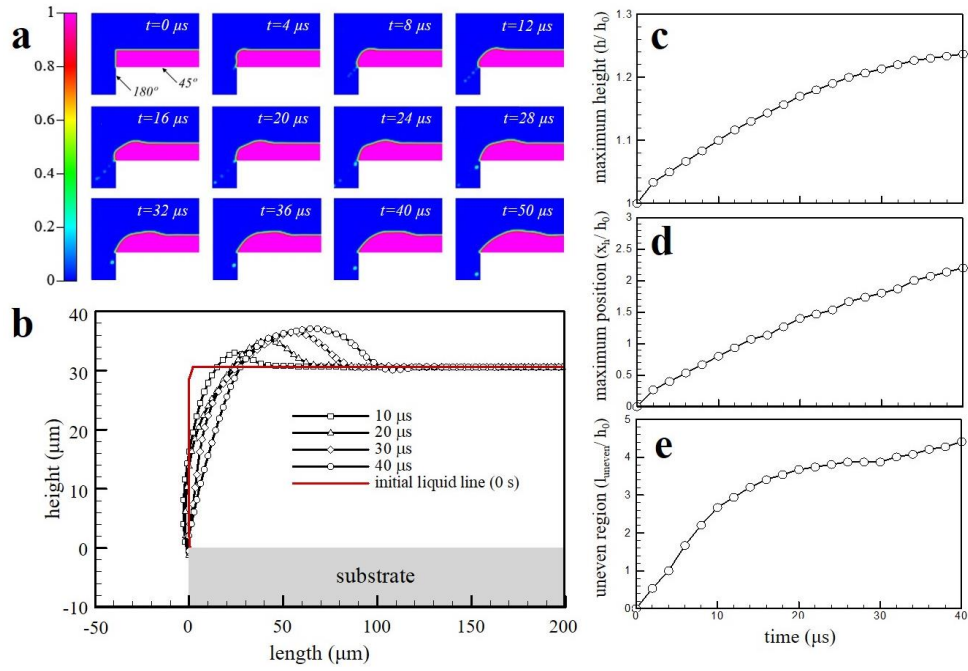


Figure S8. (a) Coating fluid behavior over time at the edge of the substrate under a substrate surface contact angle of 45° and a side contact angle of 180° , (b) surface profile under the different wetting condition, (c) maximum height, (d) maximum position, and (e) uneven region analysis of the surface unevenness at the edge of substrate under the different wetting condition.

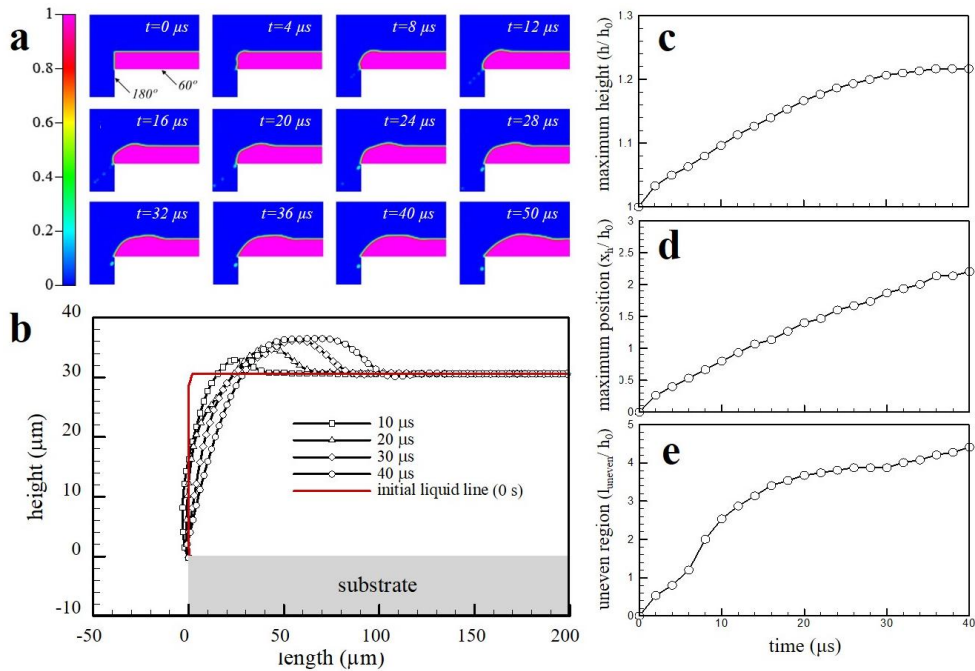


Figure S9. (a) Coating fluid behavior over time at the edge of the substrate under a substrate surface contact angle of 60° and a side contact angle of 180° , (b) surface profile under the different wetting condition, (c) maximum height, (d) maximum position, and (e) uneven region analysis of the surface unevenness at the edge of substrate under the different wetting condition.

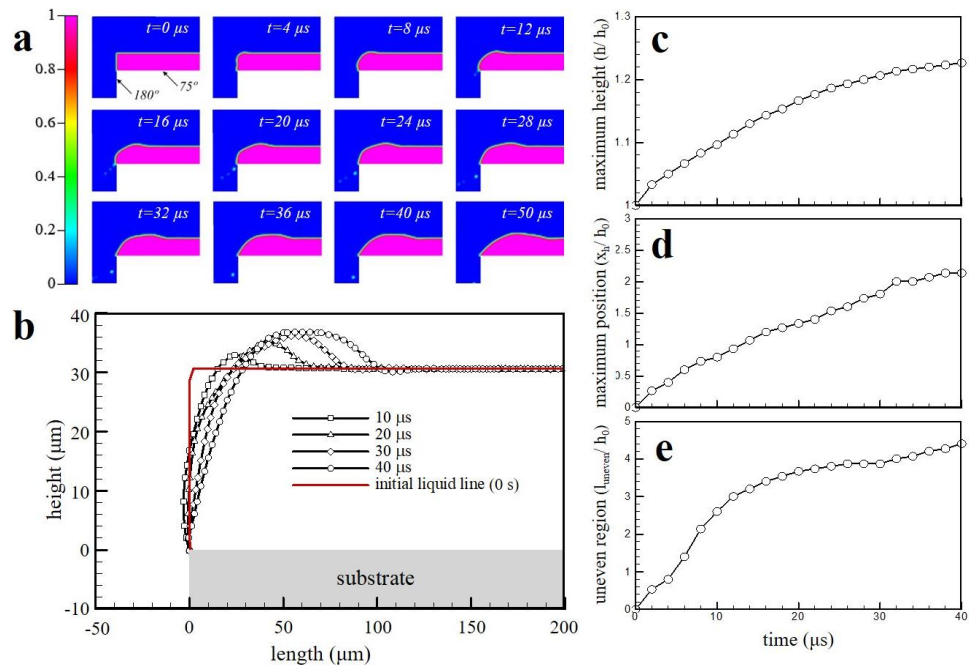


Figure S10. (a) Coating fluid behavior over time at the edge of the substrate under a substrate surface contact angle of 75° and a side contact angle of 180° , (b) surface profile under the different wetting condition, (c) maximum height, (d) maximum position, and (e) uneven region analysis of the surface unevenness at the edge of substrate under the different wetting condition.